

# Integrated analysis identifies a long non-coding RNAs-messenger RNAs signature for prediction of prognosis in hepatitis B virus-hepatocellular carcinoma patients

Zhenzi Bai, MD, Hongyan Li, MD, Chenghua Li, MD, Chuanlun Sheng, MD, Xiaonan Zhao, MM\* 

## Abstract

Hepatitis B virus (HBV) infection is a leading cause of hepatocellular carcinoma (HCC), but HBV-HCC related prognosis signature remains rarely investigated. This study was to identify an integrated long non-coding RNAs-messenger RNAs (lncRNA-mRNA) signature for prediction of overall survival (OS) and explore their underlying functions.

One RNA-sequencing dataset (training set,  $n=95$ ) and one microarray dataset E-TABM-36 (validation set,  $n=44$ ) were collected. Least absolute shrinkage and selection operator analysis was performed to identify an lncRNA-mRNA prognosis signature. The OS difference of patients in the high-risk and low-risk risk groups was evaluated by Kaplan–Meier curve. Area under the receiver operating characteristic curve (AUC), Harrell concordance index (C-index) calculation, and multivariate analyses with clinical characteristics were used to determine the prognostic ability. Furthermore, a coexpression network was constructed to interpret the functions.

Nine signature genes (3 lncRNAs and 6 mRNAs) were selected to generate the risk score model. Patients belonging to the high-risk group showed a significantly shorter survival than those of the low-risk group. The prediction accuracy of the risk score for 5-year OS was 0.936 and 0.905 for the training set and validation set, respectively. Also, this risk score was independent of various clinical variables for the prognosis prediction. Incorporation of the risk score remarkably increased the predictive power of the routine clinical prognostic factors (vascular invasion status, tumor recurrence status) (AUC=0.942 vs 0.628; C-index=0.7997 vs 0.6908). Furthermore, lncRNA insulin-like growth factor 2 antisense RNA (IGF2-AS) and long intergenic non-protein coding RNA 342 (LINC00342) were predicted to exert tumor suppression effects by regulating homeobox D1 (HOXD1) and secreted frizzled related protein 5 (SFRP5), respectively; while lncRNA raphilin Rho GTPase binding protein 1 antisense RNA 1 (RHPN1-AS1) may possess carcinogenic potential by promoting the transcription of chromobox 2 (CBX2), cell division cycle 20 (CDC20), matrix metalloproteinase 12 (MMP12), stratifin (SFN), tripartite motif containing 16 (TRIM16), and uroplakin 3A (UPK3A). These mRNAs may be associated with cell proliferation or apoptosis related pathways.

This study may provide a novel, effective prognostic biomarker, and some therapeutic targets for HBV-HCC patients.

**Abbreviations:** AUC = area under the ROC, CBX2 = chromobox 2, CDC20 = cell division cycle 20, C-index = Harrell concordance index, DAVID = Database for Annotation, Visualization, and Integrated Discovery, DEGs = differentially expressed genes, DELs = differentially expressed lncRNAs, EMBL-EBI = The European Bioinformatics Institute, FC = fold change, FDR = false discovery rate, GO = Gene Ontology, HBV = hepatitis B virus, HCC = hepatocellular carcinoma, HGNC = HUGO Gene Nomenclature Committee, HOXD1 = homeobox D1, HR = hazard ratio, IGF2-AS = insulin-like growth factor 2 antisense RNA, KEGG = Kyoto Encyclopedia of Genes and Genomes, KM = Kaplan–Meier, LASSO = least absolute shrinkage and selection operator,

Editor: Undurti N. Das.

ZB and HL have contributed equally to this work.

Funding: None.

Availability of data and materials: The RNA-seq data were downloaded from the TCGA (<https://portal.gdc.cancer.gov/>) and EMBL-EBI (<https://www.ebi.ac.uk/arrayexpress/>).

Ethics approval and consent to participate: As the data used in this study was downloaded from EMBL-EBI or TCGA database and no human experiment was involved in this study, there was no informed consent.

Consent for publication: Not applicable.

The authors have no conflicts of interest to disclose.

The datasets generated during and/or analyzed during the current study are publicly available.

Infectious Department, the Third Hospital of Jilin University, Changchun, China.

\* Correspondence: Xiaonan Zhao, Infectious Department, the Third Hospital of Jilin University, Changchun 130033, China (e-mail: zhaonx@jlu.edu.cn).

Copyright © 2020 the Author(s). Published by Wolters Kluwer Health, Inc.

This is an open access article distributed under the terms of the Creative Commons Attribution-Non Commercial License 4.0 (CCBY-NC), where it is permissible to download, share, remix, transform, and buildup the work provided it is properly cited. The work cannot be used commercially without permission from the journal.

How to cite this article: Bai Z, Li H, Li C, Sheng C, Zhao X. Integrated analysis identifies a long non-coding RNAs-messenger RNAs signature for prediction of prognosis in hepatitis B virus-hepatocellular carcinoma patients. *Medicine* 2020;99:40(e21503).

Received: 22 December 2019 / Received in final form: 11 June 2020 / Accepted: 30 June 2020

<http://dx.doi.org/10.1097/MD.00000000000021503>

LIMMA = Linear Models for Microarray Data, LINC00342 = long intergenic non-protein coding RNA 342, lncRNAs = long non-coding RNAs, MMP12 = matrix metalloproteinase 12, mRNAs = messenger RNAs, NSCLC = non-small cell lung cancer, OS = overall survival, PCC = Pearson correlation coefficients, RHPN1-AS1 = rhotaxilin Rho GTPase binding protein 1 antisense RNA 1, ROC = receiver operating characteristic curve, RT-PCR = reverse transcription-polymerase chain reaction, SFN = stratifin, SFRP5 = secreted frizzled related protein 5, TCGA = The Cancer Genome Atlas, TRIM16 = tripartite motif containing 16, UPK3A = uroplakin 3A, VEGF = vascular endothelial growth factor.

**Keywords:** coexpression, hepatitis B virus, hepatocellular carcinoma, overall survival, signature

## 1. Introduction

Although great progressions have been made in screening, diagnosis, and treatment of liver cancer, it remains the leading cause of cancer death worldwide.<sup>[1]</sup> Prior exposure to hepatitis B virus (HBV) infection is believed as the major contributor to the development of hepatocellular carcinoma (HCC).<sup>[2,3]</sup> Therefore, novel prognostic biomarkers are still required for patients with HBV-associated HCC in order to closely monitor the high-risk patients to improve their prognosis.

Recently, there have some molecular models developed to predict the overall survival (OS) of patients with HBV-HCC, including messenger RNAs (mRNAs) and long non-coding RNAs (lncRNAs). For example, Yang et al<sup>[4]</sup> used the microarray dataset GSE14520 and univariate/multivariate Cox proportional hazards regression analysis to identify a 3-gene (SPP2, CDC37L1, and ECHDC2) prognostic signature. This signature can significantly divide the patients into the high-risk group (lower OS ratio) and low-risk group (lower mortality). Liu et al<sup>[5]</sup> utilized the RNA-sequencing data extracted from The Cancer Genome Atlas (TCGA) database to screen a 9-lncRNA combination (DGCR9, GBA3, HCG4, NAT8B, NBR2, PART1, RFPL1S, SLC22A18AS, and TCL6), which was demonstrated to significantly distinguish the OS ratio between the high-risk and low-risk groups, with the accuracy of 95.3%. Zhu et al<sup>[6]</sup> identified a 9-gene signature (consisting of ZC2HC1A, MARCKSL1, PTGS1, CDKN2B, CLEC10A, PRDX3, PRKCH, MPEG1, and LMO2) using microarray and TCGA datasets and demonstrated this signature was independent from clinical parameters for prediction of OS in HBV-related HCC patients. However, specific prognostic signatures for HBV-HCC patients remain rarely reported. Furthermore, some scholars attempted to integrate the lncRNAs and mRNAs as a prognostic signature for other cancers<sup>[7,8]</sup> and the results implicated the multi-mRNA/lncRNA-based classifier may be more effective than the risk score model constructed only by multi-lncRNA or multi-mRNA in prediction of OS.<sup>[9,10]</sup> Therefore, it may be more clinically valuable to develop an integrated prognostic signature for HBV-HCC.

In this study, we aimed to collect the transcriptome profiles (including lncRNAs and mRNAs) from TCGA and The European Bioinformatics Institute (EMBL-EBI) and develop a new multi-RNA-type signature for the prediction of OS in HBV-HCC patients.

## 2. Materials and methods

### 2.1. Data source

The mRNA sequencing data (level 3, normalized expression values) were downloaded from TCGA database (<https://portal.gdc.cancer.gov>) on August 25, 2019 using the search word of

“hepatocellular carcinoma.” A total of 423 samples (including 373 HCC samples and 50 normal liver controls) were obtained, in which only 95 HCC samples were used for the following analysis because they were HBV-positive and had complete clinical prognosis information. This dataset was used as the training set.

In addition, EMBL-EBI database (<https://www.ebi.ac.uk/arrayexpress/>) was also searched to screen another dataset with HBV-HCC samples. As a result, a microarray dataset under accession number E-TABM-36<sup>[11]</sup> was obtained, in which 44 of 65 samples were HBV-positive and had survival information. This dataset was used as the validation set.

### 2.2. Screening of mRNAs and lncRNAs differentially expressed

The annotation of lncRNAs and protein-coding mRNAs were obtained from HUGO Gene Nomenclature Committee (HGNC; <http://www.genenames.org/>) database.<sup>[12]</sup> Differentially expressed genes (DEGs) and lncRNAs (DELs) between HBV-HCC samples and normal controls were identified by using the Linear Models for Microarray Data (LIMMA) method (version 3.34.7; <https://bioconductor.org/packages/release/bioc/html/limma.html>).<sup>[13]</sup> False discovery rate (FDR) < 0.05 and at least 2-fold change (FC) ( $|\log_2FC| > 1$ ) were chosen as the cut-off criteria. Heat maps were created using pheatmap R package (version: 1.0.8; <https://cran.r-project.org/web/packages/pheatmap>) to observe the clustering effects of DEGs and DELs.

### 2.3. Identification of an lncRNA-mRNA signature for prognosis prediction in the training dataset

Univariate Cox regression analysis was performed for the 95 samples in the training dataset to preliminarily examine DEGs and DELs that were significantly associated with OS (log-rank  $P$ -value < .05) using the survival package (version 2.41-1; <http://bioconductor.org/packages/survival/>). Then, multivariate Cox regression analysis was used to screen independent prognostic DEGs and DELs. In order to further capture a more perfect signature combination, least absolute shrinkage and selection operator (LASSO), an L1 norm minimization statistical model, was applied for the genes screened by multivariate Cox regression analysis using the penalized package (version, 0.9-5; <http://bioconductor.org/packages/penalized/>).<sup>[14,15]</sup> The risk score model of lncRNA-mRNA signature was established based on the expression of lncRNAs-mRNAs ( $Exp_{lncRNA-mRNA}$ ) and their LASSO Cox regression coefficients ( $\sum \beta_{lncRNA-mRNA}$ ): Risk score =  $\sum \beta_{lncRNA-mRNA} \times Exp_{lncRNA-mRNA}$ .

According to the median risk score, the HBV-HCC patients were divided into the low-risk and high-risk groups. Kaplan–Meier (KM) survival curve was drawn to measure the OS

differences between the high-risk and low-risk groups. The area under the receiver operating characteristic (ROC) curve (AUC) was utilized to evaluate the prognostic accuracy of this risk score.

#### 2.4. Validation of the prognostic lncRNA-mRNA signature in the validation dataset

According to corresponding median risk score in the validation dataset, patients were also divided into the high-risk and low-risk groups. The KM survival and ROC curves were then analyzed to further validate the prognostic effects of the risk score.

#### 2.5. The prognostic independence of this lncRNA-mRNA signature

Univariate and multivariate Cox regression analyses were conducted to determine whether the prognostic ability of this risk score was independent of other clinical pathological characteristics using the survival package (version 2.41-1; <http://bioconductor.org/packages/survival/>). The threshold of statistical significance was set as log-rank  $P < .05$ . The association between the risk score and other independent clinical characteristics was further estimated by stratification analysis, nomogram formulation using rms package (version 5.1-2; <https://cran.r-project.org/web/packages/rms/index.html>) and Harrell concordance index (C-index) calculation by survcomp package in R (version 1.34.0; <http://www.bioconductor.org/packages/release/bioc/html/survcomp.html>).

#### 2.6. Identification of lncRNA-mRNA signature associated functions

To understand possible roles of DELs, an lncRNA-mRNA coexpressed network was constructed. The correlation between

DELs and DEGs was estimated using tcor.test function (<https://stat.ethz.ch/R-manual/R-devel/library/stats/html/cor.test.html>) in R, by which Pearson correlation coefficients (PCC) were obtained. The  $PCC > 0.5$  was set for the criterion and the network was visualized using Cytoscape (version 3.4; [www.cytoscape.org/](http://www.cytoscape.org/)). The functions of DEGs in this network were predicted using the Database for Annotation, Visualization, and Integrated Discovery (DAVID) (v6.8; <http://david.abcc.ncifcrf.gov/>), including Gene Ontology (GO) biological process terms and Kyoto Encyclopedia of Genes and Genomes (KEGG) pathways. Statistical significance was set at  $P < .05$  for the function enrichment results.

### 3. Results

#### 3.1. Identification of survival-related mRNAs and lncRNAs

After removal of the expression median value of zero, 13,454 mRNAs, and 1238 lncRNAs were finally re-annotated by HGNC database. The DEGs and DELs were analyzed in 95 HBV-HCC tissues and 50 controls of the training dataset using the LIMMA method. Based on the given threshold, 682 differentially expressed RNAs were identified, including 640 DEGs and 42 DELs (Fig. 1A). These differentially expressed RNAs were demonstrated to obviously cluster the samples into 2 groups (Fig. 1B).

Univariate Cox regression analysis was performed for these 682 differentially expressed RNAs to explore whether they were survival-related. As a result, 128 of them (including 108 DEGs and 20 DELs) were found to meet the statistical threshold value. Then, multivariate Cox regression analysis was carried out to identify independent survival factors, which yielded 28 genes, including 15 DEGs and 13 DELs. To narrow down the panel, LASSO model was implemented, by which 9 of 28 genes were considered as the optimal prognostic signature, including 6 DEGs (CBX2, chromobox 2; CDC20, cell division cycle 20; MMP12,

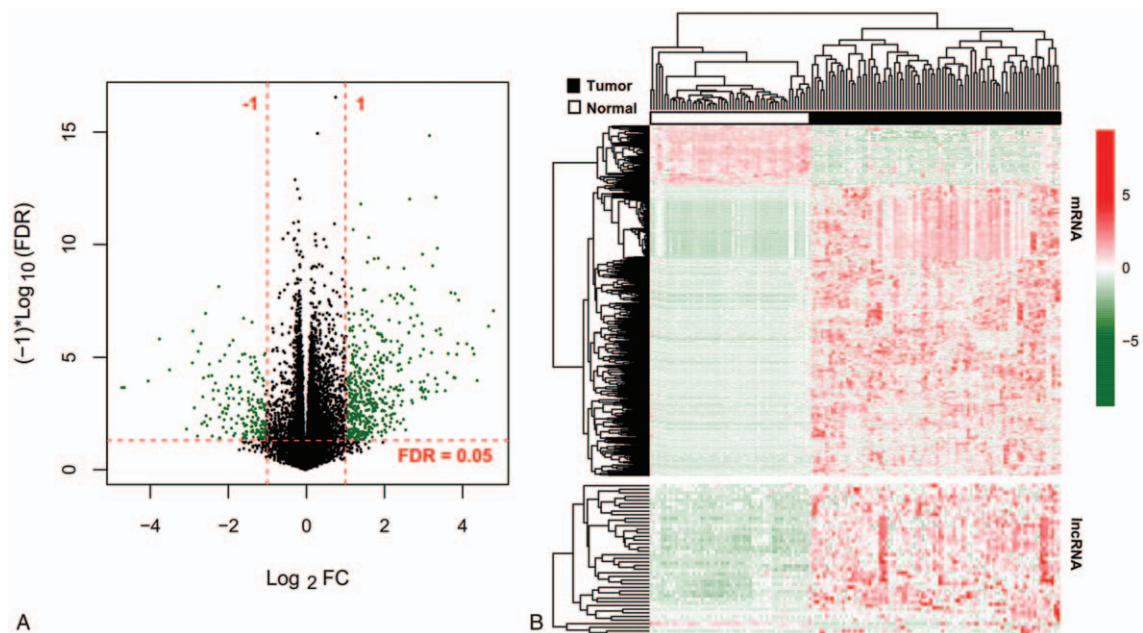


**Figure 1.** Identification of differentially expressed RNAs between 95 HBV-HCC tissues and 50 controls. A, Volcano plot was drawn to indicate the distribution of differentially expressed RNAs. Green dots represent significant RNAs. B, Heat map of differentially expressed lncRNAs and mRNAs. Red, high expression; green, low expression. FC=fold change; FDR=false discovery rate; lncRNAs=long non-coding RNAs; mRNAs=messenger RNAs.

**Table 1**  
Prognostic signature screened.

Symbol	Chromosome location	Type	Univariate Cox regression analysis			LASSO coefficient
			HR	95%CI	P-value	
IGF2-AS	11p15.5	lncRNA	0.813	0.525–0.959	3.50E–02	–0.1223
LINC00342	2q11.1	lncRNA	0.705	0.394–0.864	2.40E–02	–0.0165
RHPN1-AS1	8q24.3	lncRNA	2.920	1.499–5.708	1.70E–04	0.0470
CBX2	17q25.3	mRNA	1.850	1.221–2.800	3.70E–03	0.1661
CDC20	1p34.2	mRNA	1.490	1.153–1.921	2.30E–03	0.0996
MMP12	11q22.2	mRNA	1.410	1.086–1.829	9.90E–03	0.1589
SFN	1p36.11	mRNA	1.320	1.129–1.552	5.60E–04	0.1155
TRIM16	17p12	mRNA	1.570	1.220–2.021	4.60E–04	0.1736
UPK3A	22q13.31	mRNA	1.290	1.106–1.494	1.00E–03	0.2254

CI=confidence interval; HR=hazard ratio; LASSO=least absolute shrinkage and selection operator.

matrix metalloproteinase 12; SFN, stratifin; TRIM16, tripartite motif containing 16; and UPK3A, uroplakin 3A) and 3 DELs (IGF2-AS, insulin-like growth factor 2 antisense RNA; LINC00342, long intergenic non-protein coding RNA 342; and RHPN1-AS1, raphilin Rho GTPase binding protein 1 antisense RNA 1) (Table 1).

As shown in Table 1, the hazard ratio (HR) and LASSO coefficients of IGF2-AS and LINC00342 were respectively <1 and negative, which indicated they may be tumor suppressor genes and their high expression predicted good OS; while contrast results were obtained for the remaining genes, suggesting they were oncogenic and anti-survival. These explanations were proved by the KM survival curve analysis (Fig. 2).

### 3.2. Prognostic assessment of the risk score in the training dataset

A risk score model was developed using the expression and LASSO coefficients according to the corresponding formula described in the method. Then, it was calculated for each patient. Using a cut-off point of median risk score, the patients fell into 2 categories: high-risk group ( $\geq$ median; n = 48) and low-risk group (<median; n = 47) (Fig. 3A). KM survival curve analysis showed the OS was significantly differential between the high-risk group and low-risk group (HR = 5.887;  $P = 2.379 \times 10^{-6}$ ), with the high-risk group exhibiting lower OS ratio (Fig. 3B). ROC analysis also suggested the risk score model had a good prognostic value (1-year OS: AUC = 0.938; 3-year OS: AUC = 0.939; 5-year OS: AUC = 0.936) (Fig. 3C).

### 3.3. External validation of the prognostic value of the risk score

The predictive performance of the 9-gene signature screened in the training set was further evaluated using another validation set collected from EMBL-EBI database. The patients in the validation set were also classified into the high-risk (n = 22) and low-risk groups (n = 22) according to its cut-off (Fig. 3D). Consistent with the result of the training dataset, OS was also shown to be significantly lower in the high-risk group than that in the low-risk group (HR = 4.141;  $P = 1.707 \times 10^{-3}$ ) (Fig. 3E). KM-AUC values were 0.898, 0.917, and 0.905 for 1-year, 3-year, and 5-year OS (Fig. 3F).

### 3.4. Independence evaluation of this risk score

To evaluate the independent power of this risk score, univariate and multivariate Cox regression analyses were also performed

using the clinicopathological factors and our risk score. The results revealed that our risk score was independent of other clinicopathological factors to predict the OS (Table 2). Furthermore, we also conducted risk stratification analyses in HBV-HCC patients with vascular invasion and tumor recurrence status which were also independent factors in multivariate analysis. As shown in Fig. 4, patients in the high-risk group had significantly worse OS than those in the low-risk group in subgroups of without vascular invasion ( $P = 1.664 \times 10^{-4}$ ), vascular invasion ( $P = 5.507 \times 10^{-4}$ ), without tumor recurrence ( $P = 1.875 \times 10^{-3}$ ) and tumor recurrence ( $P = 3.635 \times 10^{-4}$ ). These stratification results indicated that the lncRNA-mRNA based prognostic model had better predictive performance than these 2 independent clinical risk factors. To further compare the prediction advantage of the risk score to clinical factors, time-dependent ROC analysis and C-index calculation were executed. As expected, the AUC (0.921) and C-index (0.7727) of lncRNA-mRNA based risk score were higher than those of vascular invasion (AUC = 0.642; C-index = 0.6401) and tumor recurrence status (AUC = 0.658; C-index = 0.6288) alone, and even combination of them (AUC = 0.628; C-index = 0.6908) (Fig. 5A). Of course, integration of the risk score with clinical factors may be the most effective for prediction of OS (AUC = 0.942; C-index = 0.7997), which can also be observed in the calibration curve of the nomogram, showing a good agreement between predicted and observed OS (Fig. 5B and C).

### 3.5. Functional annotation for signature genes

In order to interpret the biological functions and pathways of the signature lncRNAs and mRNAs, a coexpression network was first established using all DELs and DEGs and then the relevant DEGs were subjected to DAVID database. Based on the cut-off point of  $PCC > 0.5$ , 437 coexpression pairs were obtained between 35 DELs and 230 DEGs (such as IGF2-AS-HOXD1 [homeobox D1], LINC00342-SFRP5 [secreted frizzled related protein 5], RHPN1-AS1-CBX2/CDC20/SFN/TRIM16/UPK3A/MMP12) which were used to construct a coexpression network (Fig. 6). The enriched KEGG pathways for these genes in the network included “hsa04110:Cell cycle (CDC20, SFN),” “hsa04115:p53 signaling pathway (SFN),” and “hsa04114:Oocyte meiosis (CDC20).” The main enriched GO biological processes included “GO:0051301~cell division (CDC20),” “GO:0001822~kidney development (UPK3A),” “GO:0045893~positive regulation of transcription, DNA-templated (TRIM16),” “GO:0016925~protein sumoylation (CBX2),” and “GO:0008285~negative regulation of cell proliferation (SFRP5)” (Table 3).

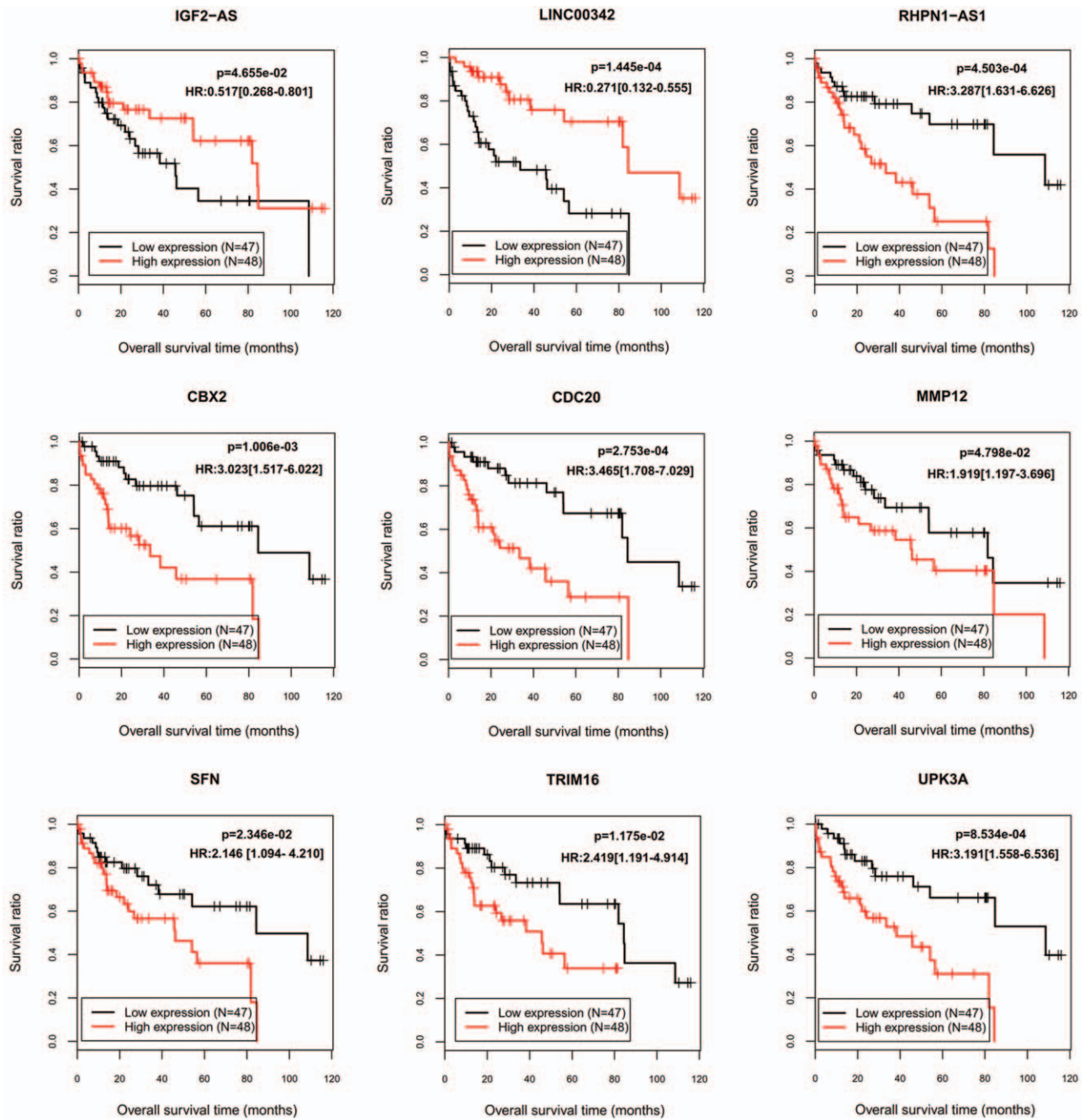
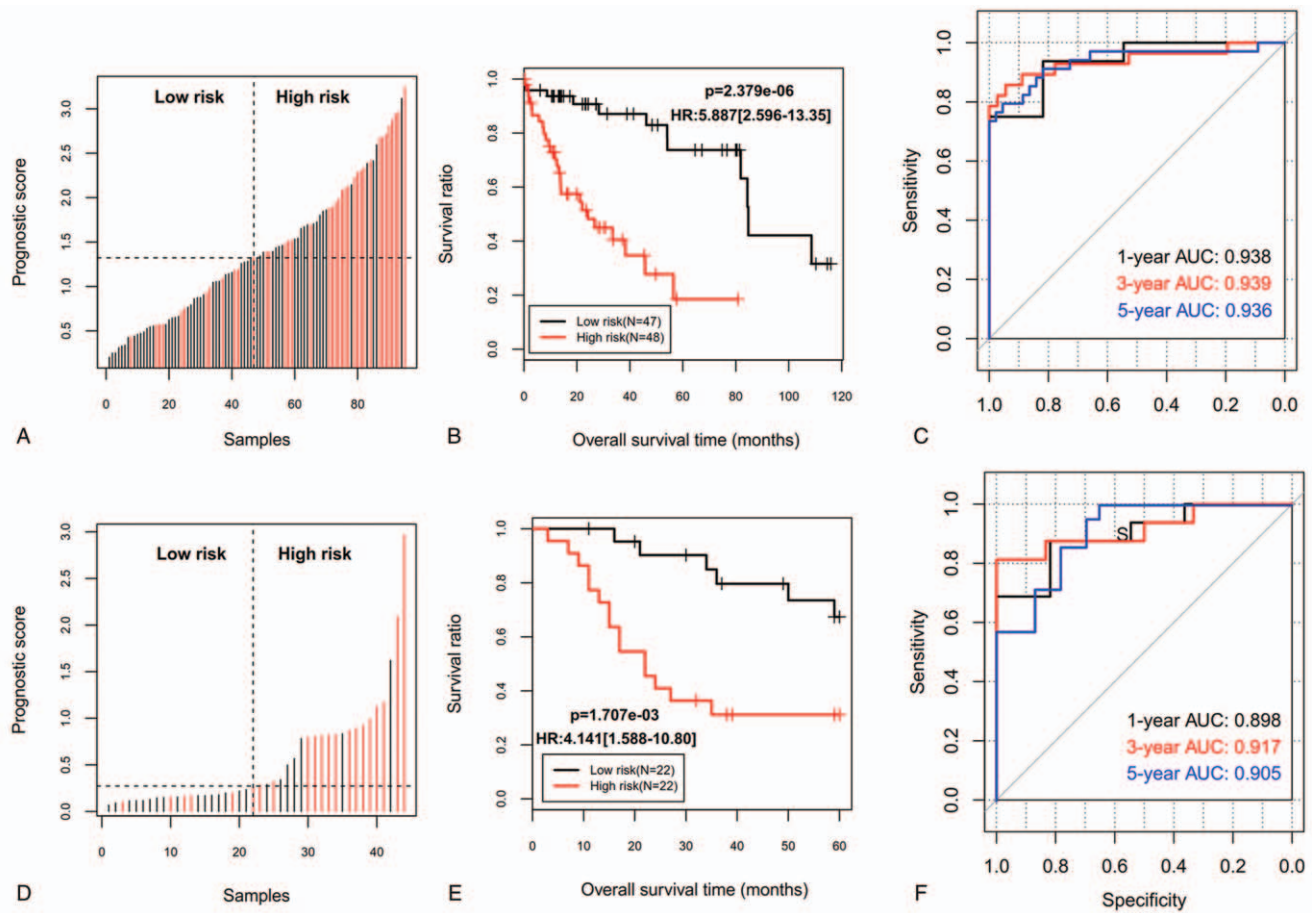


Figure 2. Kaplan-Meier plots to display the prognosis values of 9 signature genes. HR=hazard ratio.

#### 4. Discussion

Using 2 datasets, we identified and validated a novel integrated lncRNA-mRNA signature (3-lncRNA: IGF2-AS, LINC00342 and RHPN1-AS1; 6-mRNA: CBX2, CDC20, MMP12, SFN, TRIM16 and UPK3A) for prediction of OS in HBV-positive HCC patients. This 9-lncRNA/mRNA signature was demonstrated to be more accurate for prognostic prediction when compared with only lncRNAs or mRNAs (AUC=0.921 vs 0.759 or 0.819, respectively; C-index=0.7727 vs 0.6598 or 0.7434, respectively), which was in line with the study of Wang et al.<sup>[16]</sup> Stratified by vascular invasion and tumor recurrence status, this integrated lncRNA-mRNA signature still significantly distinguished the OS

ratio of the high-risk and low-risk groups, suggesting our molecular signature can be used to further refine these 2 clinical prognostic systems.<sup>[17,18]</sup> The prognostic benefit of the risk score given to the vascular invasion and tumor recurrence status can also be seen from the AUC of time-dependent ROC curve (0.942 vs 0.642 or 0.658, respectively), C-index (0.7997 vs 0.6401 or 0.6288, respectively), and calibration curve of the nomogram. Although TNM stage has been extensively believed as an important predictor to evaluate patients' survival time, univariate, and multivariate Cox regression analyses in this study did not find a statistical significance with OS, including whole TNM stage and individual pathologic M, T, and N stage, implying the



**Figure 3.** The prognosis of patients in high-risk and low-risk groups divided according to the risk score. A, D: Distribution of risk score of training set (A) and validation set (D); B, E: Kaplan–Meier survival analysis between patients at a low and high risk of death for the training set (B) and validation set (E); C, F: time dependent ROC curves at 1-, 3-, and 5-years for the training set (C) and validation set (F). AUC = the area under the ROC curve; HR = hazard ratio; ROC = receiver operating characteristic curve.

limited prognostic power of TNM staging, which was in accordance with the previous studies.<sup>[10,19]</sup>

IGF2-AS was reported to be upregulated in a dose-dependent manner in retinal pigment epithelial ARPE-19 cells that underwent high-glucose induced apoptosis. After IGF2-AS was

silenced, the apoptosis of ARPE-19 cells was ameliorated.<sup>[20]</sup> This protective effects of IGF2-AS inhibition on cell apoptosis was also observed in dorsal root ganglion neuron.<sup>[21]</sup> Inhibition of IGF2-AS was also demonstrated to augment proliferation and invasion in myocardial microvascular endothelial cells of Goto-Kakizaki

**Table 2**  
Univariate and multivariate analysis to confirm the independence of signature.

Features	TCGA (N = 95)	Univariate Cox		Multivariate Cox	
		HR (95% CI)	P-value	HR (95%CI)	P-value
Age (mean ± SD, yr)	61.21 ± 14.90	1.039 (1.008–1.070)	1.26E–02	1.000 [0.972–1.029]	9.99E–01
Gender (male/female)	58/37	1.296 (0.661–2.544)	4.49E–01	–	–
Neoplasm histologic grade (G1/G2/G3)	12/47/36	1.071 (0.646–1.775)	7.91E–01	–	–
Pathologic M (M0/M1/-)	60/2/33	1.088 (0.919–10.28)	6.33E–01	–	–
Pathologic N (N0/N1/-)	59/2/34	1.178 (0.849–16.23)	1.47E–01	–	–
Pathologic T (T1/T2/T3/T4/-)	38/33/21/2/1	1.131 (0.752–1.700)	5.55E–01	–	–
Pathologic stage (Stage I/II/III/IV)	36/30/22/2	1.037 (0.697–1.543)	8.57E–01	–	–
Vascular invasion (Yes/No/-)	38/47/10	2.421 (1.232–4.756)	8.12E–03	3.513 [1.638–7.538]	1.25E–03
Tumor recurrence (Yes/No/-)	38/57	2.321 (1.217–4.429)	8.56E–03	2.248 [1.089–4.636]	2.83E–02
Risk score status (high/low)	47/48	5.887 [2.596–13.35]	2.38E–06	7.498 [3.121–18.02]	6.65E–06
Death (dead/alive)	38/57	–	–	–	–
Overall survival time (mean ± SD, mo)	32.25 ± 29.77	–	–	–	–

CI = confidence interval; HR = hazard ratio; SD = standard deviation; TCGA = The Cancer Genome Atlas.

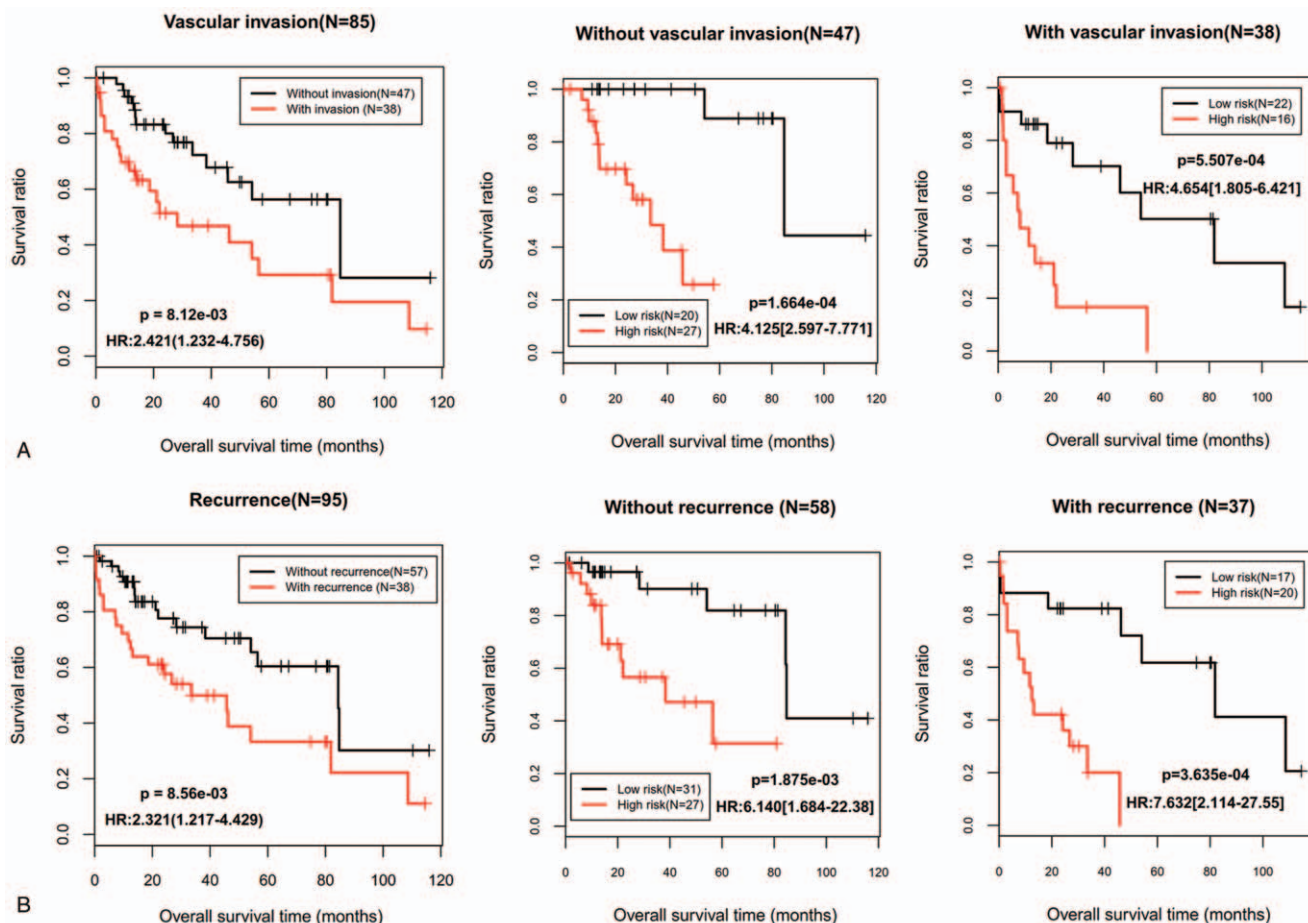
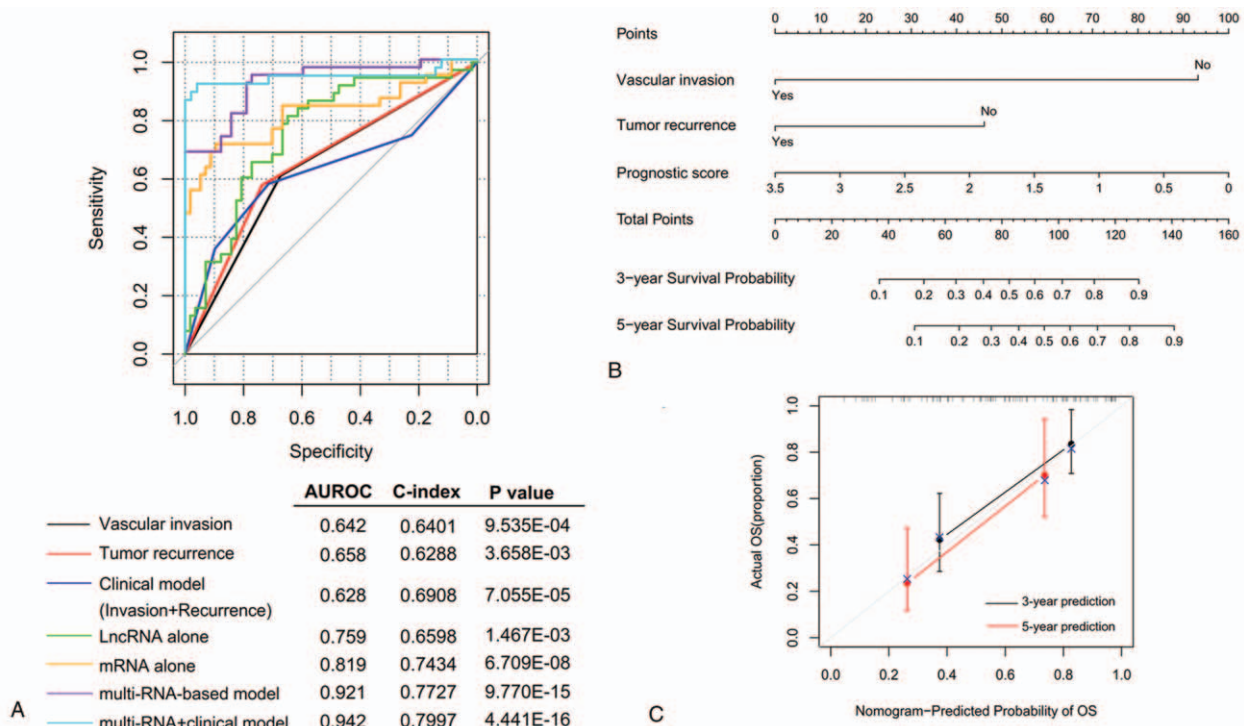


Figure 4. Kaplan–Meier survival analyses for the patients with vascular invasion (A) and tumor recurrence status (B) in the training dataset. HR=hazard ratio.

rats by upregulating pro-angiogenic IGF2 and vascular endothelial growth factor (VEGF) at both molecular and protein levels.<sup>[22]</sup> These findings suggested IGF2-AS may be a tumor suppressor. This hypothesis had also been implicated in some cancers. For example, Chen et al<sup>[23]</sup> observed lentivirus-mediated overexpression of IGF2-AS suppressed prostate cancer cell proliferation and invasion in vitro, and xenograft development in vivo via downregulation of IGF2. Similarly, Zhang et al<sup>[24]</sup> detected upregulation of IGF2-AS had anti-cancer effects by inhibiting non-small cell lung cancer (NSCLC) cell proliferation, migration in vitro, and explant growth in vivo through reducing oncogenic IGF2, VEGF, and bFGF (basic fibroblast growth factor). Moreover, high expression of IGF2-AS was significantly correlated with longer OS in patients with NSCLC. In agreement with these studies, we also found IGF2-AS may be a protective factor for HBV-HCC (HR < 1), showing the OS was higher in patients having high levels than those with lower expressions of IGF2-AS. However, its downstream mechanisms remain not well understood in addition to pro-angiogenic factors. In this study, we predicted IGF2-AS may regulate HOXD1. A previous study showed small interfering RNA-mediated knockout of HOXD1 remarkably enhanced breast cancer cell migration, invasion and cell adhesion,<sup>[25]</sup> indicating HOXD1 may also be a tumor suppressor gene, not similar to its other family members.<sup>[26]</sup> Thus, as a protective response mechanism, high expressed IGF2-

AS may inhibit the development of HBV-HCC by upregulating HOXD1.

Although several studies had proved lncRNA LINC00342 promoted proliferation, colony formation, migration, and invasion for NSCLC<sup>[27]</sup> and infantile hemangioma,<sup>[28]</sup> our results showed patients with high expression of LINC00342 had longer OS than those with lower expression of LINC00342, implying LINC00342 may have an anti-tumor activity in HBV-HCC specifically. Furthermore, we predicted LINC00342 may exert tumor suppression effects by downregulating SFRP5. SFRP5 is an endogenous inhibitor of Wnt signaling (activation of which had been linked to HBV-induced carcinogenesis<sup>[29,30]</sup>). Thus, SFRP5 may function as a tumor suppressor gene. This hypothesis had been verified in several cancers. For example, the study results of Xu et al<sup>[31]</sup> showed overexpression of SFRP5 significantly suppressed the proliferation, colony formation, and invasion, but induced cell cycle arrest and apoptosis of prostate cancer cells, compared with vector-transfected control cells. In vivo studies also confirmed that overexpression of SFRP5 significantly blocked the growth of xenograft tumors and increased terminal deoxynucleotidyl transferase biotin-dUTP nick end labeling-positive cells (apoptosis). Sheng et al<sup>[32]</sup> reported epigenetic silencing of SFRP5 promoted the metastasis and invasion of chondrosarcoma by expression inhibition and Wnt signaling pathway activation. Xie et al<sup>[33]</sup> revealed HBV X



**Figure 5.** Comparison of the prediction advantage of risk score with clinical factors. A, Time-dependent ROC curves; B, a nomogram containing clinical factors and risk score; C, the calibration plots for predicting 3- and 5-year overall survival. AUROC=the area under the receiver operating characteristic curve; OS=overall survival.

protein induced the downregulation of SFRP5 to trigger the development of HCC, which was significantly correlated with overexpression of DNA methyltransferase 1. In accordance with these studies, we also identified SFRP5 was lower expressed in

HBV-HCC samples and SFRP5 was enriched in process of negative regulation of cell proliferation.

There was increasing evidence that RHPN1-AS1 was a critical modulator of cancers. It was significantly upregulated in various

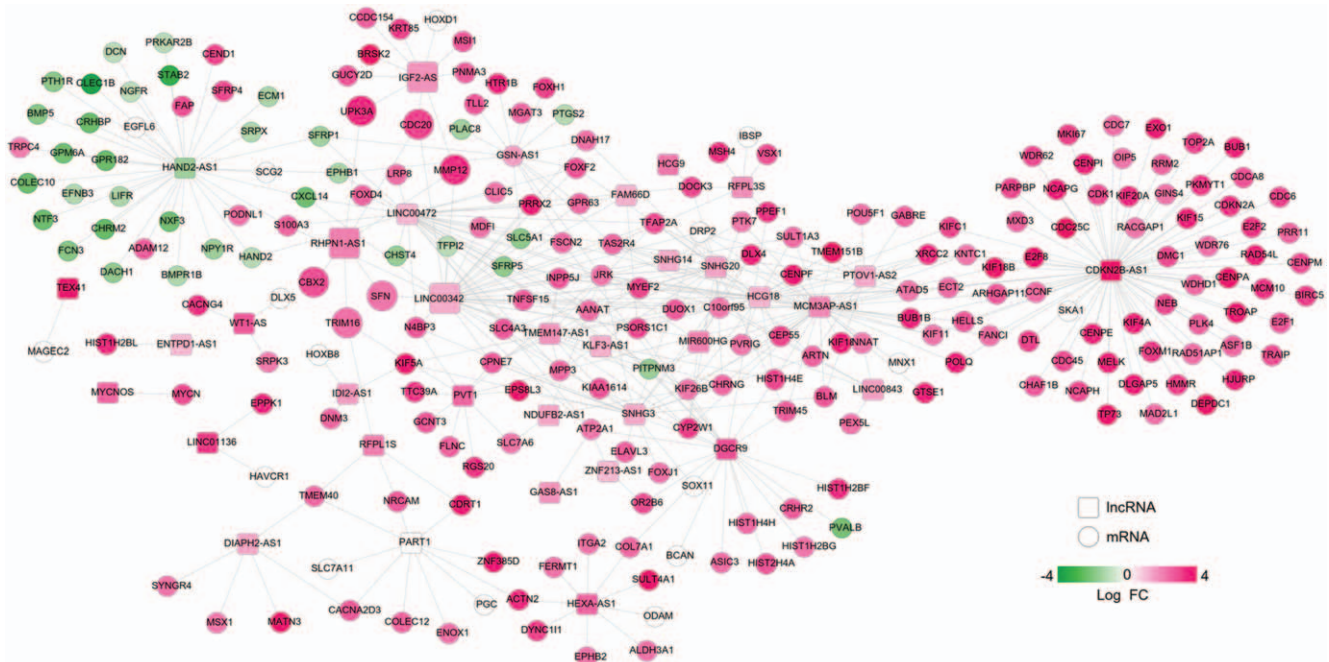


**Figure 6.** A coexpression network established between differentially expressed lncRNAs and mRNAs. Red, upregulated; green, downregulated. FC=fold change; lncRNAs=long non-coding RNAs; mRNAs=messenger RNAs.



**Table 3****Function enrichment for genes in the coexpression network.**

Category	Term	P-value	Genes
Biology process	GO:0007018~microtubule-based movement	4.170E-10	DYNC111, KIFC1, KIF4A, KIF11, KIF5A, DNAH17, KIF15, KIF18A, KIF18B, CENPE, RACGAP1, KIF26B, KIF20A
	GO:0007062~sister chromatid cohesion	5.980E-10	CENPM, KIF18A, KNTC1, CENPF, CDC20, CENPE, BIRC5, CENPI, CDCA8, MAD2L1, CENPA, BUB1, BUB1B, SKA1
	GO:0051301~cell division	7.030E-10	CDC7, CDC6, KIFC1, CDK1, KIF11, CCNF, KNTC1, BRSK2, KIF18B, CENPF, BIRC5, CDC20, CENPE, CDC25C, NCAPH, CDCA8, MAD2L1, OIP5, NCAPG, BUB1, BUB1B, SKA1, HELLS
	GO:0007067~mitotic nuclear division	1.870E-08	CDC6, CDK1, KIF11, CCNF, KIF15, KNTC1, BRSK2, PKMYT1, CENPF, BIRC5, CDC20, CEP55, CDC25C, OIP5, BUB1, BUB1B, SKA1, HELLS
	GO:0034080~CENP-A containing nucleosome assembly	1.050E-06	CENPM, CENPA, HJURP, OIP5, HIST1H4E, HIST2H4A, CENPI, HIST1H4H
	GO:0006260~DNA replication	4.630E-06	EXO1, CDC7, CDK1, CDC6, CDC45, BLM, DTL, RRM2, GINS4, CDC25C, MCM10, CHAF1B
	GO:0000086~G2/M transition of mitotic cell cycle	6.330E-05	PRKAR2B, CDK1, PLK4, FOXM1, BRSK2, PKMYT1, BIRC5, CDC25C, MELK, HMMR
	GO:0006281~DNA repair	2.100E-04	EXO1, CDK1, XRCC2, RAD51AP1, BLM, FANCI, FOXM1, PARPBP, POLQ, DMC1, RAD54L, CHAF1B
	GO:0007059~chromosome segregation	2.210E-04	KIF11, HJURP, OIP5, CENPF, CENPE, SKA1, TOP2A
	GO:0008283~cell proliferation	2.490E-04	CDK1, MKI67, DLGAP5, E2F8, KIF15, ITGA2, CENPF, DACH1, CDC25C, MCM10, TRAP1, DLX5, BUB1, BUB1B, MELK
	GO:0000082~G1/S transition of mitotic cell cycle	3.190E-04	CDC7, CDK1, CDC6, CDC45, CDKN2A, RRM2, PKMYT1, MCM10
	GO:0006334~nucleosome assembly	8.080E-04	HIST1H2BL, HIST1H2BF, CENPA, HIST1H2BG, HIST1H4E, ASF1B, HIST2H4A, HIST1H4H
	GO:0051726~regulation of cell cycle	1.029E-03	E2F2, DTL, FOXM1, CCNF, PRR11, CENPF, PKMYT1, CDC25C
	GO:0060021~palate development	2.790E-03	MSX1, HAND2, DLX5, FOXF2, TFAP2A, EPHB2
	GO:0007411~axon guidance	4.210E-03	EFNB3, KIF5A, DLX5, ARTN, NGFR, EPHB1, KIF26B, EPHB2
	GO:0001822~kidney development	4.751E-03	SOX11, CENPF, TFAP2A, DCN, UPK3A, TP73
	GO:0007155~cell adhesion	5.901E-03	IBSP, EGFL6, FERMT1, PTK7, ITGA2, BCAN, ACTN2, CHST4, STAB2, SRPX, COL7A1, FAP, TROAP, ADAM12
	GO:0001525~angiogenesis	7.714E-03	NRCAM, PTGS2, HAND2, FAP, STAB2, ECM1, EPHB1, SCG2, EPHB2
	GO:0001501~skeletal system development	8.074E-03	MATN3, SOX11, DLX5, PTH1R, BCAN, BMPR1B, BMP5
	GO:0030198~extracellular matrix organization	1.266E-02	IBSP, MATN3, COL7A1, EGFL6, FOXF2, BCAN, ITGA2, DCN
	GO:0045893~positive regulation of transcription, DNA-templated	1.449E-02	E2F1, BLM, SOX11, FOXM1, TRIM16, TP73, MYCN, FOXH1, CDKN2A, SFRP1, HAND2, DLX5, FOXF2, TFAP2A
	GO:0043065~positive regulation of apoptotic process	1.459E-02	PNMA3, CDKN2A, SFRP1, PTGS2, SFRP4, NGFR, ECT2, TOP2A, MELK, TP73
	GO:0042493~response to drug	1.568E-02	CDK1, HTR1B, SFRP1, PTGS2, CENPF, ITGA2, LRP8, RAD54L, TP73, ALDH3A1
	GO:0016925~protein sumoylation	1.672E-02	CDCA8, CDKN2A, BLM, BIRC5, CBX2, TOP2A
	GO:0006974~cellular response to DNA damage stimulus	1.703E-02	BLM, DTL, WDR76, ATAD5, POLQ, MCM10, TOP2A, TP73
	GO:0010628~positive regulation of gene expression	1.888E-02	E2F1, CDK1, ODAM, HAND2, POU5F1, SOX11, SFRP4, TFAP2A, MYCN
	GO:0008285~negative regulation of cell proliferation	3.001E-02	SFRP5, CDC6, CDKN2A, MSX1, SFRP1, PTGS2, PTH1R, SFRP4, TFAP2A, TP73, BMP5
KEGG pathway	hsa04110:Cell cycle	4.310E-09	E2F1, CDC7, CDC6, CDK1, E2F2, PKMYT1, CDC20, SFN, CDC25C, CDC45, CDKN2A, MAD2L1, BUB1, BUB1B
	hsa05203:Viral carcinogenesis	1.157E-03	CDK1, CDKN2A, HIST1H2BL, HIST1H2BF, HIST1H2BG, HIST1H4E, ACTN2, CDC20, HIST2H4A, HIST1H4H
	hsa04115:p53 signaling pathway	1.582E-03	CDK1, CDKN2A, RRM2, SFN, GTSE1, TP73
	hsa04114:Oocyte meiosis	1.356E-02	CDK1, MAD2L1, BUB1, PKMYT1, CDC20, CDC25C
	hsa04914:Progesterone-mediated oocyte maturation	2.491E-02	CDK1, MAD2L1, BUB1, PKMYT1, CDC25C

GO = Gene Ontology, KEGG = Kyoto Encyclopedia of Genes and Genomes.

cancer cells and tissues (including uveal melanoma,<sup>[34]</sup> breast cancer,<sup>[35]</sup> head and neck squamous cell carcinoma,<sup>[36]</sup> cervical cancer,<sup>[37]</sup> and HCC<sup>[38,39]</sup>) compared with controls. Knockdown of RHPN1-AS1 significantly inhibited cancer cell proliferation, migration, and invasion in vitro and reduced tumor growth in xenograft models in vivo.<sup>[36-40]</sup> Moreover, RHPN1-AS1 was revealed to be a significant and independent predictor of prognosis, showing that patients with low expression of

RHPN1-AS1 had much longer OS than those with high expression of RHPN1-AS1,<sup>[38-40]</sup> including HCC. Our results seemed to be consistent with these studies, which also showed RHPN1-AS1 was high expressed in HBV-HCC patients and associated with poor OS. The above studies have attempted the downstream mechanisms of RHPN1-AS1 in cancers, consisting of activation of epithelial-to-mesenchymal transition<sup>[36,40]</sup> or modulation of miR-299-3p/FGF2,<sup>[37]</sup> miR-485/CDCA5,<sup>[38]</sup> miR-

596/IGF2BP2<sup>[39]</sup> axes, but it remains completely unclear. In this study, we predicted RHPN1-AS1 may promote the transcription of 6 prognostic genes (CBX2, CDC20, MMP12, SFN, TRIM16, and UPK3A). Existing studies also indicated 4 of 6 genes played oncogenic functions in HCC. For example, Mao et al<sup>[41]</sup> used immunohistochemical staining to find CBX2 expression was higher in HCC tissues than that of adjacent liver tissues and associated with poor prognosis in HCC patients. Knockdown of CBX2 inhibited the proliferation and increased apoptosis of HCC cells. Using the TCGA dataset, Liao et al<sup>[42]</sup> also identified CBX2 as one member of a prognostic signature for HCC patients, with lower OS in patients having high expression of CBX2 by KM survival curve analysis. Li et al<sup>[43]</sup> performed immunohistochemistry in 132 matched tissues to demonstrate CDC20 expression was upregulated in HCC tissues. High expression levels of CDC20 were positively correlated with the expression of proliferation marker Ki-67. CDC20 siRNA decreased cell proliferation and increased cell cycle arrest at G2/M-phase. Several bioinformatic analyses of microarray or TCGA datasets also revealed CDC20 was a hub gene for the development of HCC and overexpression of CDC20 in HCC tissues accounted for poorer OS in HCC patients,<sup>[44,45]</sup> including HBV-HCC.<sup>[46]</sup> PCR analysis determined MMP-12 mRNA was significantly elevated in tumor liver tissues of HCC patients compared with non-tumor and normal liver tissues.<sup>[47]</sup> Overexpression of MMP-12 mRNA was significantly correlated with poor overall survival for HCC patients in an independent manner.<sup>[47,48]</sup> Wang et al<sup>[49]</sup> screened SFN as an up-regulated gene in HCC and high expression level of SFN was associated with worse prognosis (HR = 1.777; adjusted *P*-value = .005). In accordance with these studies, we also found CBX2, CDC20, MMP12, and SFN were risk factors for the poor OS in HBV-HCC samples (HR > 1). Most of them were enriched in cell cycle, proliferation or apoptosis related biological processes or pathways. A recent study found TRIM16 may be a tumor suppressor in HCC, knockdown of which promoted epithelial-mesenchymal transition and then cell migration and invasion *in vitro* and *in vivo*.<sup>[50]</sup> However, in our study, we identified TRIM16 was upregulated in HBV-HCC and positively associated with shorter OS. These inconsistent results may be possibly resulted from the difference of dry and wet experiments (quantitative reverse transcription-polymerase chain reaction [RT-PCR]). Furthermore, there were also studies on gastric cancer to illustrate upregulated TRIM16 could promote cell invasion and migration,<sup>[51]</sup> suggesting TRIM16 may have dual functions in cancer. Thus, the expression and roles of TRIM16 should be further validated in the future. No studies reported the roles of UPK3A in HCC until now, but the related research on bladder cancer may indirectly clarify its possible oncogenic functions: UPK3A levels in serum, plasma, and urine were shown to be elevated in patients compared with healthy controls and associated with muscle-invasive status, high grade, lymphovascular invasion, and cancer-specific mortality.<sup>[52,53]</sup>

There were still some limitations in this study. First, the sample size of our collected datasets from public databases was not large due to the fact that this study specifically focused on HBV-HCC, not overall HCC. More newly hospitalized HBV-HCC patients and controls in our institution should be prospectively included confirm the OS prediction ability of our lncRNA-mRNA signature. Second, the clinical information (such as therapies) were not detail for patients in TCGA database and thus, the

influences of other clinical factors on the prognosis of HBV-HCC patients have to be confirmed using new case series. Third, quantitative PCR should be performed to examine the expression of lncRNAs and mRNAs at RNA levels, while western blotting or immunohistochemistry should be conducted to determine the protein levels of mRNAs because RNA-sequencing or microarray results seemed not to be completely consistent with these wet experiments. Fourth, although we preliminarily predicted the functions of lncRNAs in HBV-HCC based on the coexpression mechanisms with mRNAs, their interaction relationships still need experimental confirmation, such as coimmunoprecipitation. Furthermore, the roles of lncRNAs and mRNAs for HBV-HCC also require *in vitro* (overexpression or knockdown of lncRNAs and mRNAs, followed by cell proliferation, apoptosis, invasion, and metastasis assays) and *in vivo* validation (tumor growth in xenograft models). Fifth, lncRNAs can act as competing endogenous RNAs to indirectly regulate mRNAs by sponging miRNAs.<sup>[37–39]</sup> Several studies also suggested miRNAs were important biomarkers for prognosis prediction in HCC patients.<sup>[54–57]</sup> Therefore, lncRNA-miRNA-mRNA signature may also be effective for prognosis prediction, which may be a potential direction in our subsequent studies. Sixth, the prognosis potential of other DEGs (such as Dickkopf-1, another important wnt pathway gene<sup>[58]</sup>) and DELs that were not included in the risk score should be independently confirmed using clinical samples to supplement our conclusions.

## 5. Conclusion

Through a series of bioinformatics analyses, we preliminarily established a 9-lncRNA/mRNA risk score model which may be potentially effective and independent biomarkers for prediction of OS in HBV-HCC patients by dividing them into the high-risk and low-risk groups and then guide therapeutic schedule. Furthermore, in routine clinical practice, high-risk patients of cancer-related death may be better recognized by the nomogram that incorporated the risk score model and clinical prognostic systems (vascular invasion and tumor recurrence status). By constructing the lncRNA-mRNA coexpression and function annotation analysis, we predicted high expressed IGF2-AS and LINC00342 may exert tumor suppression effects by regulating HOXD1 and SFRP5, respectively; while high expressed RHPN1-AS1 may possess carcinogenic potential by promoting the transcription of CBX2, CDC20, MMP12, SFN, TRIM16, and UPK3A. These mRNAs were all associated with cell proliferation or apoptosis related pathways. These results may also provide underlying therapeutic targets for HBV-HCC.

## Author contributions

**Conceptualization:** Zhenzi Bai, Xiaonan Zhao.

**Data curation:** Zhenzi Bai, Hongyan Li.

**Formal analysis:** Zhenzi Bai.

**Investigation:** Chenghua Li, Chuanlun Sheng.

**Methodology:** Hongyan Li.

**Resources:** Chenghua Li.

**Software:** Chuanlun Sheng.

**Supervision:** Xiaonan Zhao.

**Validation:** Xiaonan Zhao.

**Writing – original draft:** Zhenzi Bai.

**Writing – review & editing:** Xiaonan Zhao.

## References

- [1] Siegel RL, Miller KD, Jemal A. Cancer statistics, 2019. *CA Cancer J Clin* 2019;69(suppl):7–34.
- [2] Yang F, Ma L, Yang Y, et al. Contribution of Hepatitis B Virus infection to the aggressiveness of primary liver cancer: a clinical epidemiological study in eastern china. *Front Oncol* 2019;9:370.
- [3] Xie Y. Hepatitis B virus-associated hepatocellular carcinoma. *Adv Exp Med Biol* 2017;1018:11–21.
- [4] Yang Y, Lu Q, Shao X, et al. Development of a three-gene prognostic signature for hepatitis b virus associated hepatocellular carcinoma based on integrated transcriptomic analysis. *J Cancer* 2018;9:1989–2002.
- [5] Liu H, Zhao P, Jin X, et al. A 9-lncRNA risk score system for predicting the prognosis of patients with hepatitis B virus-positive hepatocellular carcinoma. *Mol Med Rep* 2019;20:573–83.
- [6] Zhu GQ, Yang Y, Chen EB, et al. Development and validation of a new tumor-based gene signature predicting prognosis of HBV/HCV-included resected hepatocellular carcinoma patients. *J Transl Med* 2019;17:203.
- [7] Shi YM, Li YY, Lin JY, et al. The discovery of a novel eight-mRNA-lncRNA signature predicting survival of hepatocellular carcinoma patients. *J Cell Biochem* 2019;120:7539–50.
- [8] He SY, Xi WJ, Wang X, et al. Identification of a combined RNA prognostic signature in adenocarcinoma of the lung. *Med Sci Monit* 2019;25:3941–56.
- [9] Xiong Y, Wang R, Peng L, et al. An integrated lncRNA, microRNA and mRNA signature to improve prognosis prediction of colorectal cancer. *Oncotarget* 2017;8:85463–78.
- [10] Xiang Y, Li C, Liao Y, et al. An integrated mRNA-lncRNA signature for relapse prediction in laryngeal cancer. *J Cell Biochem* 2019;120:15883–90.
- [11] Kim SM, Leem SH, Chu IS, et al. Sixty-five gene-based risk score classifier predicts overall survival in hepatocellular carcinoma. *Hepatology* 2012;55:1443–52.
- [12] Povey S, Lovering R, Bruford E, et al. The HUGO Gene Nomenclature Committee (HGNC). *Hum Genet* 2001;109:678–80.
- [13] Ritchie ME, Phipson B, Wu D, et al. limma powers differential expression analyses for RNA-sequencing and microarray studies. *Nucleic Acids Res* 2015;43:e47.
- [14] Goeman JJ. L1 penalized estimation in the Cox proportional hazards model. *Biom J* 2010;52:70–84.
- [15] Tibshirani R. The lasso method for variable selection in the Cox model. *Stat Med* 1997;16:385–95.
- [16] Wang Z, Wu Q, Feng S, et al. Identification of four prognostic lncRNAs for survival prediction of patients with hepatocellular carcinoma. *PeerJ* 2017;5:e374.
- [17] Hu H, Han XK, Long XR, et al. Prognostic nomogram for post-surgical treatment with adjuvant TACE in hepatitis B virus-related hepatocellular carcinoma. *Oncotarget* 2016;7:58302–14.
- [18] Zhou L, Rui JA, Wang SB, et al. Risk factors of microvascular invasion, portal vein tumor thrombosis and poor post-resectional survival in HBV-related hepatocellular carcinoma. *Hepatogastroenterology* 2014;61:1696–703.
- [19] Dai W, Feng Y, Mo S, et al. Transcriptome profiling reveals an integrated mRNA-lncRNA signature with predictive value of early relapse in colon cancer. *Carcinogenesis* 2018;39:1235–44.
- [20] Yu X, Luo Y, Chen G, et al. Long noncoding RNA IGF2AS regulates high-glucose induced apoptosis in human retinal pigment epithelial cells. *IUBMB Life* 2019;71:1611–8.
- [21] Zhang X, Chen K, Song C, et al. Inhibition of long non-coding RNA IGF2AS has profound effect on inducing neuronal growth and protecting local-anesthetic induced neurotoxicity in dorsal root ganglion neurons. *Biomed Pharmacother* 2016;82:298–303.
- [22] Zhuo Z, Liu B, Bo L, et al. Inhibition of long noncoding RNA IGF2AS promotes angiogenesis in type 2 diabetes. *Biomed Pharmacother* 2017;92:445–50.
- [23] Chen Q, Sun T, Wang F, et al. Long noncoding RNA IGF2AS is acting as an epigenetic tumor suppressor in human prostate cancer. *Urology* 2019;124:310e1–8.
- [24] Zhang X, Zhang X, Hu R, et al. Prognostic implication and functional role of long noncoding RNA IGF2AS in human non-small cell lung cancer. *J Cell Biochem* 2017;doi: 10.1002/jcb.26113.
- [25] Li X, Zheng L, Zhang F, et al. STARD13-correlated ceRNA network inhibits EMT and metastasis of breast cancer. *Oncotarget* 2016;7:23197–211.
- [26] Zha Y, Ding E, Yang L, et al. Functional dissection of HOXD cluster genes in regulation of neuroblastoma cell proliferation and differentiation. *PLoS One* 2012;7:e40728.
- [27] Chen QF, Kong JL, Zou SC, et al. lncRNA LINC00342 regulated cell growth and metastasis in non-small cell lung cancer via targeting miR-203a-3p. *Eur Rev Med Pharmacol Sci* 2019;23:7408–18.
- [28] Liu Z, Kang Z, Dai Y, et al. Long noncoding RNA LINC00342 promotes growth of infantile hemangioma by sponging miR-3619-5p from HDGF. *Am J Physiol Heart Circ Physiol* 2019;317:H830–9.
- [29] Daud M, Rana MA, Husnain T, et al. Modulation of Wnt signaling pathway by hepatitis B virus. *Arch Virol* 2017;162:2937–47.
- [30] Zheng BY, Gao WY, Huang XY, et al. HBx promotes the proliferative ability of HL-7702 cells via the COX-2/Wnt/ $\beta$ -catenin pathway. *Mol Med Rep* 2018;17:8432–8.
- [31] Xu Q, Lü Z, Wang X, et al. Secreted frizzled-related protein 5 suppresses aggressive phenotype and reverses docetaxel resistance in prostate cancer. *J Investig Med* 2019;67:1009–17.
- [32] Sheng W, Zhang ZC, Shi DY, et al. Epigenetic silencing of SFRP5 promotes the metastasis and invasion of chondrosarcoma by expression inhibition and Wnt signaling pathway activation. *Chem Biol Interact* 2018;296:1–8.
- [33] Xie Q, Chen L, Shan X, et al. Epigenetic silencing of SFRP1 and SFRP5 by hepatitis B virus X protein enhances hepatoma cell tumorigenicity through Wnt signaling pathway. *Int J Cancer* 2014;135:635–46.
- [34] Lu L, Yu X, Zhang L, et al. The Long Non-Coding RNA RHPN1-AS1 promotes uveal melanoma progression. *Int J Mol Sci* 2017;18:226.
- [35] Zhu P, Li Y, Li P, et al. c-Myc induced the regulation of long non-coding RNA RHPN1-AS1 on breast cancer cell proliferation via inhibiting P53. *Mol Genet Genomics* 2019;294:1219–29.
- [36] Qiu X, Lei Z, Wang Z, et al. Knockdown of lncRNA RHPN1-AS1 inhibits cell migration, invasion and proliferation in head and neck squamous cell carcinoma. *J Cancer* 2019;10:4000–8.
- [37] Duan H, Li X, Chen Y, et al. lncRNA RHPN1-AS1 promoted cell proliferation, invasion and migration in cervical cancer via the modulation of miR-299-3p/FGF2 axis. *Life Sci* 2019;13:116856.
- [38] Zhang X, Yan Z, Wang L, et al. STAT1-induced upregulation of lncRNA RHPN1-AS1 predicts a poor prognosis of hepatocellular carcinoma and contributes to tumor progression via the miR-485/CDCA5 axis. *J Cell Biochem* 2020;doi: 10.1002/jcb.29689.
- [39] Fen H, Hongmin Z, Wei W, et al. RHPN1-AS1 drives the progression of hepatocellular carcinoma via regulating miR-596/IGF2BP2 axis. *Curr Pharm Des* 2020;25:4630–40.
- [40] Zheng S, Lv P, Su J, et al. Silencing of the long non-coding RNA RHPN1-AS1 suppresses the epithelial-to-mesenchymal transition and inhibits breast cancer progression. *Am J Transl Res* 2019;11:3505–17.
- [41] Mao J, Tian Y, Wang C, et al. CBX2 regulates proliferation and apoptosis via the phosphorylation of YAP in hepatocellular carcinoma. *J Cancer* 2019;10:2706–19.
- [42] Liao X, Wang X, Huang K, et al. Integrated analysis of competing endogenous RNA network revealing potential prognostic biomarkers of hepatocellular carcinoma. *J Cancer* 2019;10:3267–83.
- [43] Li J, Gao JZ, Du JL, et al. Increased CDC20 expression is associated with development and progression of hepatocellular carcinoma. *Int J Oncol* 2014;45:1547–55.
- [44] Zhuang L, Yang Z, Meng Z. Upregulation of BUB1B, CCNB1, CDC7, CDC20, and MCM3 in tumor tissues predicted worse overall survival and disease-free survival in hepatocellular carcinoma patients. *Biomed Res Int* 2018;2018:7897346.
- [45] Li L, Lei Q, Zhang S, et al. Screening and identification of key biomarkers in hepatocellular carcinoma: evidence from bioinformatic analysis. *Oncol Rep* 2017;38:2607–18.
- [46] Chen Z, Chen J, Huang X, et al. Identification of potential key genes for Hepatitis B virus-associated hepatocellular carcinoma by bioinformatics analysis. *J Comput Biol* 2019;26:485–94.
- [47] Ng KT, Qi X, Kong KL, et al. Overexpression of matrix metalloproteinase-12 (MMP-12) correlates with poor prognosis of hepatocellular carcinoma. *Eur J Cancer* 2011;47:2299–305.
- [48] He MK, Le Y, Zhang YF, et al. Matrix metalloproteinase 12 expression is associated with tumor FOXP3+ regulatory T cell infiltration and poor prognosis in hepatocellular carcinoma. *Oncol Lett* 2018;16:475–82.
- [49] Wang X, Zhou X, Liu J, et al. Genome-wide investigation of the clinical implications and molecular mechanism of long noncoding RNA LINC00668 and protein-coding genes in hepatocellular carcinoma. *Int J Oncol* 2019;55:860–78.
- [50] Li L, Dong L, Qu X, et al. Tripartite motif 16 inhibits hepatocellular carcinoma cell migration and invasion. *Int J Oncol* 2016;48:1639–49.

- [51] Yan Y, Shen Z, Gao Z, et al. Long noncoding ribonucleic acid specific for distant metastasis of gastric cancer is associated with TRIM16 expression and facilitates tumor cell invasion in vitro. *J Gastroenterol Hepatol* 2015;30:1367–75.
- [52] Hideyasu T, Kazumasa M, Masaomi I, et al. High expression level of preoperative serum Uroplakin III is associated with biologically aggressive bladder cancer. *Asian Pac J Cancer Prev* 2015;16:1539–43.
- [53] Szymańska B, Matuszewski M, Dembowski J, et al. Uroplakin IIIa is a marker in bladder cancer but seems not to reflect chemical carcinogenesis. *Biomed Res Int* 2018;2018:8315410.
- [54] Li P, Fan H, He Q. Investigation of the clinical significance and prognostic value of microRNA-145 in human hepatocellular carcinoma. *Medicine (Baltimore)* 2018;97:e13715.
- [55] Zhang Y, Li Y, Jiang W, et al. The clinical significance of microRNA-122 in predicting the prognosis of patients with hepatocellular carcinoma: a meta-analysis validated by the Cancer Genome Atlas dataset. *Medicine (Baltimore)* 2019;98:e14810.
- [56] Shi W, Zhang Z, Yang B, et al. Overexpression of microRNA let-7 correlates with disease progression and poor prognosis in hepatocellular carcinoma. *Medicine (Baltimore)* 2017;96:e7764.
- [57] Elhendawy M, Abdul-Baki EA, Abd-Elsalam S. MicroRNA signature in hepatocellular carcinoma patients: identification of potential markers. *Mol Biol Rep* 2020;47:4945–53.
- [58] Watany M, Badawi R, Elkhawany W, et al. Study of Dickkopf-1 (DKK-1) gene expression in hepatocellular carcinoma patients. *J Clin Diagn Res* 2017;11:OC32–4.